Journal Homepage: http://ijcpe.uobaghdad.edu.iq
Iraqi Journal of Chemical and Petroleum Engineering
Vol. 26 No. 2 (June 2025) 1 – 10
EISSN: 2618-0707, PISSN: 1997-4884

Analysis of production characteristics and engineering measures for deep coalbed methane wells in the Ordos Basin

Zhao Zhengyan [a, c, *], Tan Xiaohua [b], Wang Xianwen [c], Tian Wei [c], Jia Youliang [c]

a School of Petroleum Engineering, Xi'an Shiyou University, Xi'an, 710065, China
b State Key Laboratory of Oil and Gas Reservoir Geology and Exploitation, Southwest Petroleum University, Xindu Road 8, Chengdu 610500, China
c Engineering Research Center of Development and Management for Low to Ultra-Low Permeability Oil & Gas Reservoirs in West China, Ministry of Education, Xi'an, 710065, China

Abstract

Given the significant differences in gas accumulation modes, coal reservoir characteristics, and gas preservation conditions for ultra-deep coalbed methane (vertical depth > 3000 m, measured depth > 5000 m), their production characteristics, flowback patterns, and flow phase classifications also vary greatly. Additionally, there are limitations in the production technologies applicable to deep reservoirs. To explore the relationship between the production characteristics of deep coalbed methane and medium-shallow coalbed methane, as well as to investigate suitable technologies for deep coalbed methane, this paper uses Well Q1 as an example and conducts research and analysis based on reservoir engineering theory. It is believed that in the vertical section of Well Q1(The depth is generally less than 3000m), the flow pattern transitions from bubbly flow to slug flow in the early stage, and with reduced water production, it is predicted to transition from transitional flow to annular flow in the later stage. In the inclined section (The depth is generally between 3000 and 4000m), slug flow predominates most of the time, while in the horizontal section (The depth is generally greater than 4000m), the flow evolves from elongated bubble flow to slug flow in the early stage, from elongated bubble flow to stratified smooth flow in the middle stage, and remains in the stratified smooth flow zone in the later stage. Furthermore, it is proposed that the insertion depth of Well Q1 should be correlated with the well deviation angle, gas production rate, and water production rate. From the perspective of gas-water ratio optimisation and energy efficiency, there should be an optimal timing for tubing insertion.

Keywords: Deep coalbed methane; Production regime; Production mode; Engineering measures; Flowback analysis; Flow pattern prediction.

Received on 28/02/2025, Received in Revised Form on 09/04/2025, Accepted on 10/04/2025, Published on 30/06/2025

https://doi.org/10.31699/IJCPE.2025.2.1

1- Introduction

In the latter half of the 20th century, T. E. Crist et al. [1] made a significant discovery in the San Juan Basin of Colorado and New Mexico, identifying the Menefee Formation within the Upper Cretaceous Mesaverde Group as containing rich coal seams with abundant coalbed methane resources. Building on this, A. H. Jones et al. [2] conducted an in-depth analysis of the production characteristics of deeply buried coalbed methane in the San Juan Basin, focusing on minimizing pressure fluctuations caused by the reciprocating motion of downhole pumps. Subsequently, Kenneth J. Johnson et al. [3] pioneered the application of gas-lift technology in coalbed methane wells within the Black Warrior Basin. Meanwhile, J. Misselbrook et al. [4] introduced an innovative process that utilized separate flow paths for water lifting, significantly enhancing gas production rates in wells affected by liquid loading issues.

Martin J. Willis et al. [5] highlighted the importance of screw pumps in coalbed methane operations due to the presence of fine particles, despite their relatively high cost for dewatering applications. To address this challenge, liquid chemical foamers were employed, offering a cost-effective solution for initial liquid unloading while facilitating efficient liquid management throughout the well's lifecycle. This approach not only increased long-term production but also reduced operational expenses.

F. E. Trevisan et al. [6] identified viscous effects as a critical factor leading to performance degradation in two-phase pumps. They developed a groundbreaking experimental program using a visual prototype constructed from original ESP (Electric Submersible Pump) components, incorporating minimal geometric modifications to mitigate the viscous effects associated with two-phase flow through such pumps. T. Denney et al. [7] emphasized the substantial time and effort typically invested in determining the optimal sizing of ESPs for specific applications, considering factors such as physical characteristics, reservoir deliverability, and operator economics. Recognizing the frequency of ESP failures, they proposed an evaluation system encompassing assessments of operating versus design points, diagnostic alerts, virtual monitoring, and sub-component threshold monitoring.

*Corresponding Author: Email: 2280044361@qq.com

D. B. Sarmiento Varela et al. [8] demonstrated the effectiveness of a hydraulic pneumatic variable-speed pump unit in a reciprocating rod lift system, providing an economical artificial lift solution that proved successful in developing coalbed methane production in Colombia. Guoqing Han et al. [9] advocated for the development of an automated data processing system utilizing advanced echo sounding technology to measure water levels in real-time. This system dynamically monitors reservoir pressure based on detected water levels, optimizing controlled-pressure production and reducing pump maintenance frequency.

Jinen Vora et al. [10] proposed a novel approach to optimize screw pump systems over the entire lifespan of coalbed methane wells, adapting to head increments and declining flow rates over time. By tailoring the screw pump system to different stages of the well's life, this method minimized cost impacts on the company. Charles Prosper et al. [11], after extensive research spanning four years in the Surat and Bowen Basins, identified screw pump (PCP) system failures as the primary cause of workovers in coalbed methane fields. To achieve sustainable economic production and maximize reserve recovery, they applied machine learning techniques to optimize production cycles in CBM wells.

Chidirim Ejim et al. [12] highlighted a defining characteristic of unconventional gas reservoirs: the rapid decline in reservoir pressure during production, which frequently leads to liquid-loading problems and reduces gas production to zero. To restore production, a method for unloading liquids was deemed essential. By assigning weights to each criterion and alternative unloading method based on their applicability to specific unconventional gas wells, they determined that multi-stage plunger lift, PAGL, plunger lift, GAPL, and continuous gas lift ranked among the top five candidates. Conversely, foam-assisted lift, tubing heating, soap sticks, SCS, and linear ESPs were identified as the least effective options.

D. B. Larson et al. [13] sought to enhance the efficiency of screw pumps in coalbed methane fields by introducing an intelligent pump selection method. Their improved screw pump selection process eliminated trial-and-error steps, ensuring consistently sized pumps without requiring functional hydraulic pump testing. Lastly, S. K. Sharan et al. [14], through studies on the Reliance coalbeds in India, proposed software simulation to optimize the placement of sucker rod guides and centralizers on sucker rod strings. This innovation minimized tubing integrity issues and significantly boosted natural gas production in India.

From these previous studies, it is evident that most research has concentrated on the design of screw pumps and medium-shallow coalbed methane reservoirs. However, for deep ultra-deep coalbed methane reservoirs, the limitations and high costs associated with rod pumps necessitate a reevaluation. Therefore, there is a pressing need to consider the intrinsic nature of deep ultra-deep coalbed methane reservoirs and develop an engineering intervention strategy tailored to their unique production characteristics.

2- General situation of the gas reservoir

To explore the gas accumulation model of deep anthracite-dominated coal-mud composite coal-rock gas and the exploration and development technology for the No. 8 coal-seam gas reservoir in the Benxi Formation, a risk exploration well, Nalin 1H, was deployed in Wushenqi. Its location is Talaiwusu Village, Suliude Township, Wushenqi, Erdos City, Inner Mongolia Autonomous Region, situated on the Yishan Slope structure of the Ordos Basin. The total drilled depth of the well is 5062 m, with a vertical depth of 3246.1 m and a horizontal section length of 1500 m. The well encountered 760 m of coal rock, 625 m of mudstone (carbonaceous mudstone and gray-black mudstone), 99 m of limestone, and 16 m of siltstone and fine sandstone. The coal seam encounter rate was 50.7%, with a gas detection peak of 78.5%.

The Nalin 1H well adopted a three-stage wellbore structure, and the production casing used 5-1/2" thick-walled tubing with a wall thickness of 10.54 mm, rated at 125V, having an internal pressure resistance of 113.8 MPa. On October 2nd, fracturing operations commenced using guar gel with proppant, fracturing 15 stages and 42 clusters, with a total proppant volume of 2920 cubic meters. The flow rate during fracturing ranged from 10 to 15 cubic meters per minute, with an average sand ratio of 12~14%. The total injected fluid volume was 36,442 cubic meters.

On October 21st, blowdown operations began, and ignition occurred immediately upon release, producing a flame height of 4-5 meters. The choke size was 6+12 mm, with a casing pressure of 2.6 MPa and liquid discharge at 300 cubic meters per day. On November 14th, the well transitioned into trial production, with the casing pressure steadily rising from 3.8 MPa to 5.9 MPa. The gas production increased from 0.9×10^4 m³/d to 5.7×10^4 m³/d, while water production ranged between 280 to 240 cubic meters per day. Subsequently, both the casing pressure and gas production gradually decreased.

Currently, the choke size is 8+12 mm, with a nozzle diameter of 18 mm, oil pressure of 2.4 MPa, and daily gas production stabilized at 3.3×10^4 m³/d. The cumulative gas production is 2.796×10^6 m³, with daily liquid production decreasing to 65 cubic meters (continuously declining). The cumulative liquid discharge is 15,142 cubic meters, achieving a return rate of 41.6%.

.

3- Production characteristics of well Q1

3.1. Analysis of production characteristics of well Q1

Deep coalbed methane (CBM) wells are characterized by high initial water production, generally producing between 300 to 400 cubic meters per day, with maximum values sometimes exceeding 500 cubic meters per day. The time to gas breakthrough is relatively short, typically

occurring within one month. Due to the contribution of free gas in the early stage and subsequent production being sustained by desorbed gas, deep CBM wells remain in a stable production phase for most of their production life, as illustrated in Fig. 1.

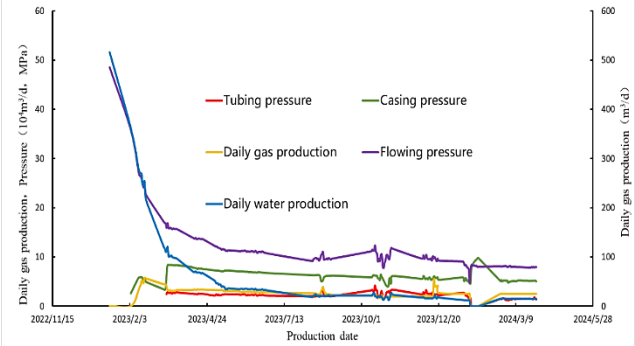

Fig. 1. Q1 Well layout diagram

The production characteristics of this well are significantly distinct from those of medium-shallow coalbed methane (CBM) wells. For shallow CBM wells, gas breakthrough typically occurs when the water production reaches its peak and begins to decline. The single-phase dewatering period is relatively long, usually lasting several months. Throughout the entire production phase, due to the sole reliance on desorbed gas for supply, the total gas content is low, resulting in a gradual increase and decrease in gas production. Additionally, prolonged pressure stabilization is required during production to maintain optimal desorption conditions. The general standard production curve for medi um-shallow CBM wells during the return drainage production phase is shown in Fig. 2.

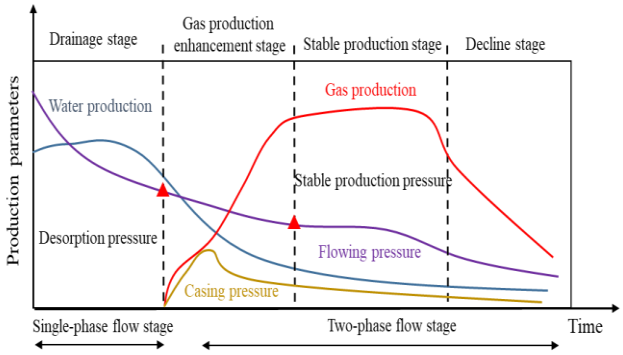

Fig. 2. Q1 Standard flowback production curve of a middle-shallow coalbed methane well

Deep coalbed methane (CBM) wells are characterized by extremely short gas breakthrough times, rapid production ramp-up, and prolonged stable production periods. They can quickly transition into a phase of low water-to-gas ratio production, significantly reducing the impact of two-phase flow. Moreover, these wells benefit from dual gas sources—free gas and desorbed gas—which enhances their productivity. As a result, deep CBM wells offer significantly greater economic benefits compared to medium-shallow CBM wells. The standard return drainage production curve for ultra-deep CBM wells is illustrated in Fig. 3.

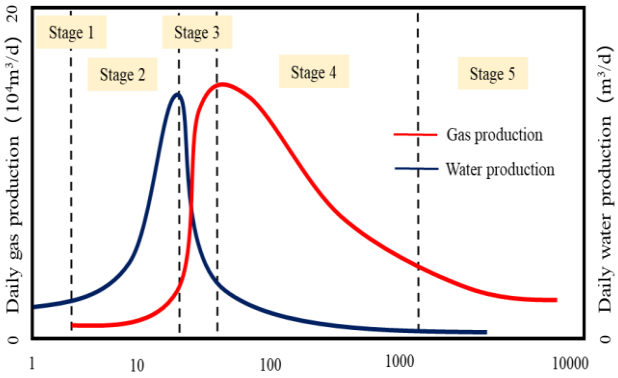

Fig. 3. Super deep coalbed methane well flowback production standard curve

Deep to ultra-deep coalbed methane (CBM) wells can generally be divided into five production stages: the post-pressurization pure liquid production stage, the gas-and-water-increase stage, the gas-increase-water-decrease stage, the gas-decrease-water-decrease stage, and the stable production-to-depletion stage. By referring to the standard production curve, Well Q1 is categorized into these stages, as shown in Table 1.

3.2. Q1 Well fracturing fluid backflow characteristics analysis

Based on the experimental study of coalbed methane fracturing fluid invasion and backflow mechanism, the microscale two-phase (gas-water) flow characteristics of coalbed reservoirs were analyzed. Combined with the actual production conditions of coalbed methane wells, a fracturing fluid backflow model for coalbed methane wells was established to analyze the backflow patterns of fracturing fluids and predict the backflow volume and its variation with production time. The flow characteristics of coalbed methane production are shown in Fig. 4.

According to Jokhio, S.A., the gas-water production ratio can be expressed as the ratio of gas relative permeability to water relative permeability, and its expression is as follows:

$$\frac{k_{rg}}{k_{rw}} = \left(\frac{B_g \mu_g}{B_w \mu_w}\right)\frac{Q_{sc}}{Q_w} \quad (1)$$

Style: K_{rg}: Gas phase relative permeability; K_{rw}: Water phase relative permeability; B_g: Volume coefficient of gas; B_w: Volume coefficient of water; μ_g: Vapor viscosity,Pa.s; μ_w: Aqueous viscosity,Pa.s.

According to the two-phase seepage theory, the left term can be expressed as a function of reservoir gas saturation:

$$f(S_g) = \frac{k_{rw}}{k_{rg}} \quad (2)$$

Style: S_g: Reservoir gas saturation.

Table 1. Q1 Well production curve stage division

	Stage1	Stage2	Stage3	Stage4	Stage5
Duration (days)	24（Post-fracturing pure liquid production phas）	（Gas and water rising stage）,The characteristics of Well Q1 are not obvious, but theoretically, the second stage exists based on the production record time.	14（Gas rising and water declining stag）	102（Gas and water declining stage）	195（Stable production stage）
Daily gas production (10^4 m^3/d)	No gas production		Maximum daily gas production: 5.74×10^4 m^3, average: 3.42×10^4 m^3	Significant decline in this stage, decreasing from 5.4×10^4 m^3 to 2.9×10^4 m^3, average: 3.53×10^4 m^3	Minimal decline in this stage, average daily decline: 0.0047×10^4 m^3, average daily gas production: 2.38×10^4 m^3
Daily liquid production (m^3/d)	Maximum daily liquid production: 516 m^3, average: 340.5 m^3		Maximum daily liquid production: 291 m^3, average: 262.7 m^3	Water production decreased from a maximum of 214 m^3 to 35 m^3	Average daily liquid decline: 0.09 m^3, average daily water production: 23.2 m^3

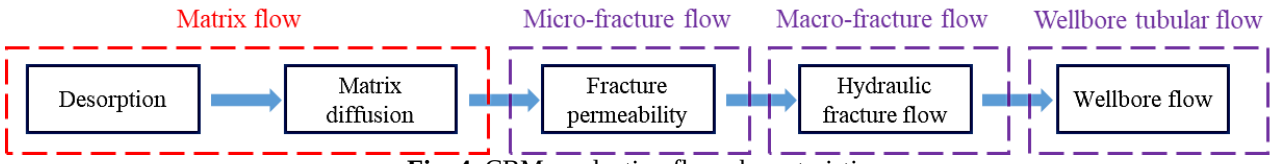

Fig. 4. CBM production flow characteristics

In accordance with the actual conditions of coalbed methane reservoirs, all the water in the reservoir is injected during fracturing. After the fracturing treatment of coalbed methane wells is completed, the area near the wellbore is fully filled with fracturing fluid, resulting in the water saturation near the wellbore approaching 1 and the gas saturation approaching 0. As the fracturing fluid is discharged, the water saturation near the wellbore of the gas well can be expressed as follows:

$$S_w = \frac{(W_{in} - W_p)B_w}{W_{in}B_{wi}} \quad (3)$$

Style: W_p: Total flowback fluid, m^3; W_{in}: Total fluid injected in fracturing, m^3; B_{wi}: The original volume coefficient of water.

Let B_{wi}=B_w, then the above formula can be rewritten as:

$$S_w = \frac{W_{in} - W_p}{W_{in}} \quad (4)$$

The gas saturation near the wellbore of the gas well can be expressed as:

$$S_g = \frac{W_p}{W_{in}} \quad (5)$$

The above equation is consistent with the expression for the fracturing fluid backflow rate:

$$R_R = \frac{W_p}{W_{in}} \quad (6)$$

By combining the above, we obtain:

$$f(R_R) = \frac{k_{rw}}{k_g} \quad (7)$$

The relationship between the backflow rate and the gas well reservoir is obtained as follows. Based on the actual pressure measurement data and production data of the gas well, the gas production, water production, and bottomhole true pressure at different production stages are determined, and the ratio of water-gas relative permeability at different production stages is calculated. Based on the total injected fluid volume during fracturing and the cumulative water production of the gas well at different production stages, the backflow rate of the gas well is calculated. Thus, the variation law of the water-gas ratio with the backflow rate is studied. Unlike shale gas backflow, due to the large amount of water production in the early stage of coalbed methane wells, a certain parameter becomes zero. Therefore, a binomial is used as an indicator for judging the backflow process. The backflow characteristics of Well Q1 are shown in Fig. 5.

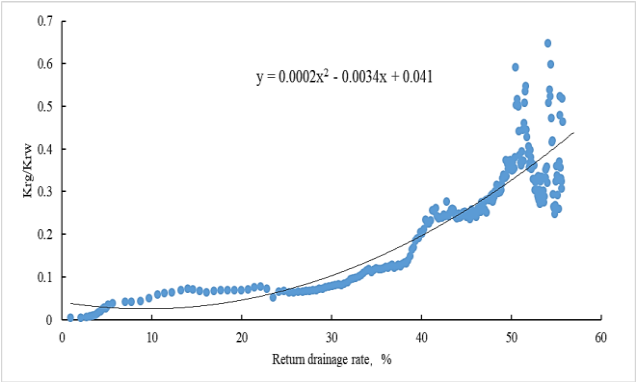

Fig. 5. Q1 Well flowback characteristics

Research shows that: the larger the first term, the faster the gas appearance, and the greater the initial liquid discharge; the smaller the second term, the later the gas appearance, and the slower the backflow. By using the binomial, the gas-water ratio under different backflow rates can be predicted, as well as the variation of water production with gas production and backflow rate. If sufficient data is available, gas wells can be classified

based on the binomial coefficients A and B to analyze the production characteristics of coalbed methane wells under different backflow patterns. Since coalbed methane wells generally experience a pure-liquid production phase after fracturing, coefficient C is usually equal to or approaches zero, and therefore is not considered in the analysis.

3.3. Q1 Well flow regime analysis

The wellbore of a horizontal well encompasses a range of angles from 0° to 90°, which can be divided into three segments: 90° to 60° as the vertical section, 60° to 30° as the inclined section, and 30° to 0° as the horizontal section. Through research and summarization, it is found that different authors have varying classifications of flow regime maps and use different units. To develop a unified flow regime map for the entire wellbore, it is necessary to standardize the coordinates and flow regimes. Therefore, all units are converted to apparent gas and liquid velocities, and the flow regime maps are reclassified for each segment. By inputting the gas and water production rates at different well depths into the corresponding flow regime maps, the flow regime characteristics at various depths can be determined.

Taking Well Q1 as an example, the average gas and water production rates during casing production, tubing production, and the later production stage, along with calculated wellbore pressures, are used to construct the flow regime distribution for the entire wellbore. The flow regime changes in the vertical section are shown in Fig. 6. As pressure decreases, the gas volume gradually increases, leading to an increase in gas phase velocity and a decrease in liquid phase velocity. The flow regime in the vertical section of this well transitions from bubble flow → slug flow, and it is predicted that it will later enter the transition flow → annular flow regime, as shown in Fig. 6.

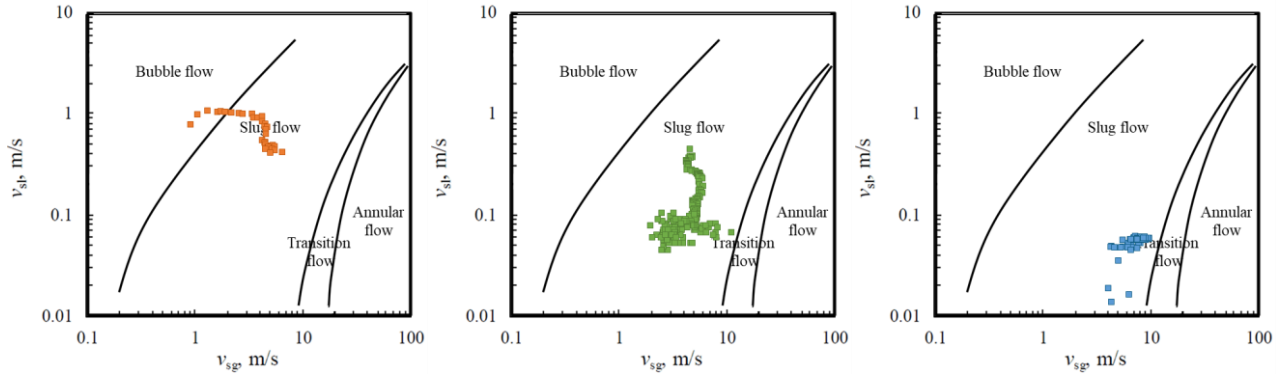

Fig. 6. Change diagram of flow pattern in the vertical section of well Q1

The flow regime changes in the inclined section are shown in Fig. 7. As the pressure decreases, the gas volume gradually increases, leading to an increase in the gas phase velocity and a reduction in the liquid phase velocity. However, the pressure variation in the inclined section is less pronounced compared to that in the vertical section. The flow regime in the inclined section of this well is identified as slug flow.

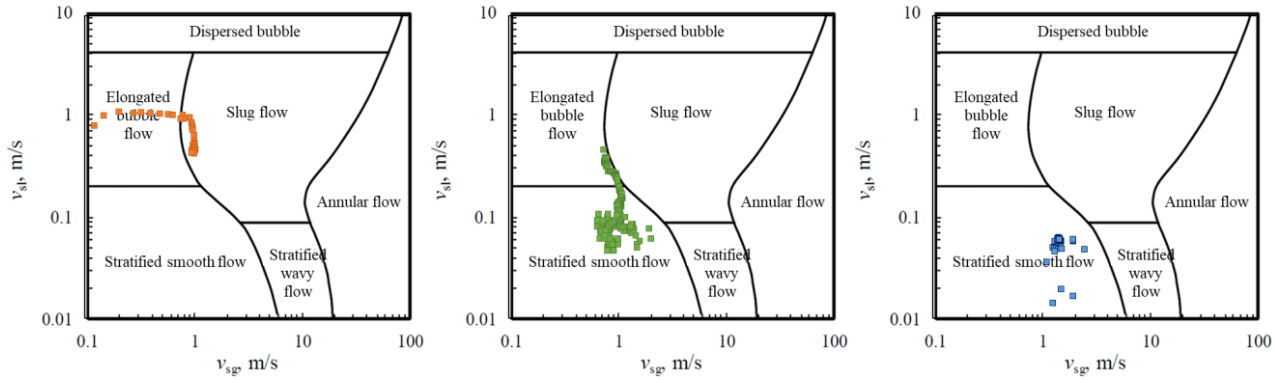

Fig. 7. Flow pattern change diagram of well Q1 inclined section

As the pressure decreases, the gas volume gradually increases, leading to an increase in the gas phase velocity and a reduction in the liquid phase velocity. In the early stage, the flow regime transitions from elongated bubble flow → slug flow; in the middle stage, it transitions from elongated bubble flow → stratified smooth flow; and in the later stage, it remains in the stratified smooth flow regime, they are shown in Fig. 8.

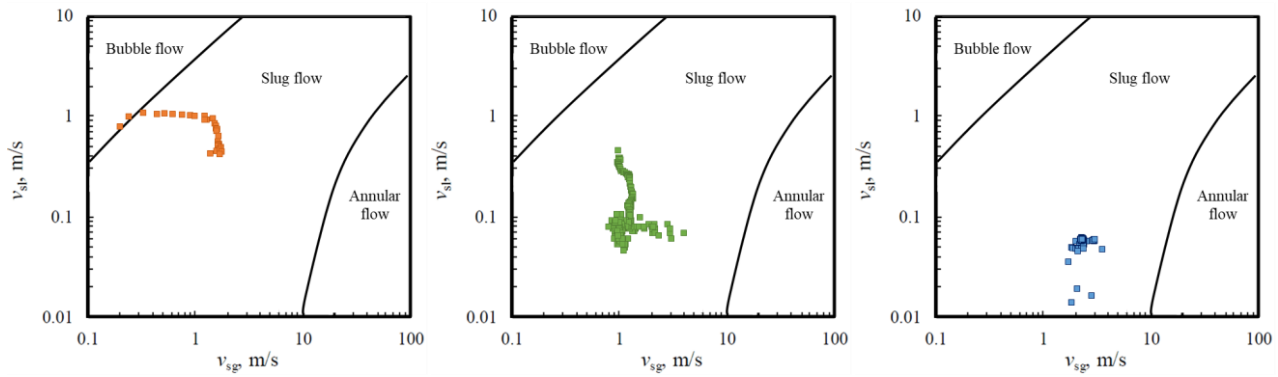

Fig. 8. Flow pattern change diagram of well Q1 inclined section

4- Process analysis of well Q1

Based on the production data, after the tubing was run in Well Q1, the gas production, water production, and pressure all entered a stable phase. This has a very positive effect on coalbed methane exploitation, indicating that the optimized tubing string design is highly adaptable and efficient in the production of deep and ultra-deep coalbed methane reservoirs. However, whether the depth of insertion and the timing of tubing deployment are optimal still requires further investigation.

4.1. Optimization of tubing depth placement

According to the critical liquid-carrying flow rate model, the critical liquid-carrying velocity of a gas well can be expressed as:

$$v_t = 4.667\left[\frac{\sigma(\rho_l-\rho_g)Q_{st}}{\mu_g^{0.2}D^{1.8}\rho_g^{1.8}}\right]^{\frac{1}{4.8}}\frac{(\sin(1.7\,\theta))^{0.38}}{0.74} \quad (8)$$

Style: v_t: Critical liquid carrying velocity, m/s; Q_{sl}: Liquid flow, m^3/d; Θ: Hole drift Angle, °.

The optimization of the gas production tubing string position also takes into account the well deviation angle, using the well deviation angle influence coefficient as an indicator to evaluate its impact on the liquid-carrying capacity of the gas well. The formula for the well deviation angle influence coefficient is as follows.

:

$$C = \frac{(\sin(1.7\,\theta))^{0.38}}{0.74} \quad (9)$$

The result of incorporating the effect of the well deviation angle into the coordinate system is shown in Fig. 9.

From the figure, it can be observed that: the well deviation angle has a significant impact on the liquid-carrying capacity of the gas well. When the well deviation angle is around 40 degrees, gas-liquid transportation becomes the most difficult. When the well deviation angle exceeds 70 degrees, the liquid-carrying capacity of the gas well aligns with that of the vertical section and begins to decrease rapidly. Therefore, the optimal insertion angle for the gas production tubing string is between 70 to 80 degrees.

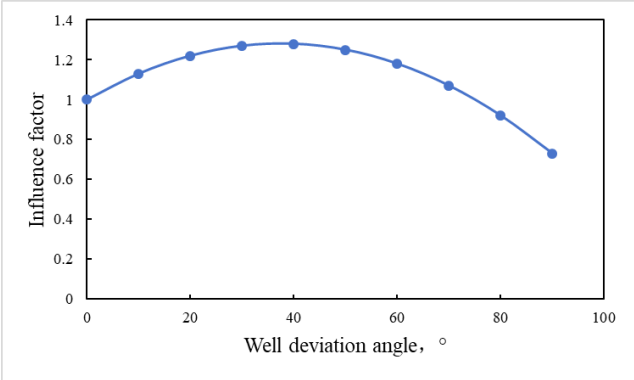

Fig. 9. Analysis of the influence coefficient of the well inclination Angle

For up-dipping and horizontal-type horizontal wells, the well deviation angle in the horizontal section of the wellbore is greater than or approximately equal to 90°. In such cases, liquid accumulation in the wellbore within the producing formation is unlikely, and the placement of the gas production tubing string is typically selected near Target Point A, where the well deviation angle is around 70° to 80°.

For down-dipping horizontal wells, liquid accumulation may occur in certain sections of the wellbore within the producing formation. The preferred objectives for placing the gas production tubing string are as follows:

(1) Under constant bottomhole pressure conditions, inserting the tubing reduces energy loss in the wellbore, which helps to unlock the gas well's production capacity.

(2) The insertion of tubing improves liquid accumulation issues in specific wellbore sections and enhances the wellbore's liquid-carrying capacity.

Taking Well Q1 as an example, the bottomhole flowing pressure before inserting the tubing was calculated to be 15.07 MPa. Assuming the gas-water ratio remains unchanged after inserting the tubing, the actual well deviation data for the gas well was used to calculate the changes in the surface pressure when inserting 2 3/8-inch tubing at different depths. The results are shown in Fig. 10.

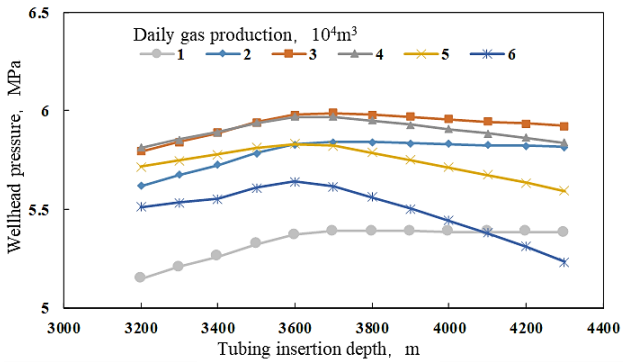

Fig. 10. Different tubing depth corresponds to wellhead pressure changes

From the figure, it can be observed that within the production range of 1~6×10⁴ m³/d, the deeper the coiled tubing is inserted, the higher the gas wellhead pressure and the greater the potential for increased production. However, when the insertion depth exceeds 3750 m, the impact of insertion depth on the wellhead pressure gradually decreases, and with further insertion, the wellhead pressure begins to decrease. After a comprehensive analysis, to effectively eliminate liquid accumulation at the bottom of the gas well while considering the insertion angle, the optimal insertion depth for the 2 3/8-inch coiled tubing in this well is determined to be 3600.0 m (vertical depth: 3246.25 m) with a well deviation angle of approximately 65.8°.

4.2. Optimization of tubing insertion timing

In coalbed methane wells, high water production and insufficient liquid-carrying capacity of the casing can lead to liquid-laden production in the wellbore, resulting in significant energy loss within the wellbore. When the reservoir energy is sufficient, the gas well can maintain liquid-laden production. However, as the reservoir energy of the coalbed methane well declines rapidly and the bottomhole pressure decreases, the wellhead pressure during liquid-laden production becomes too low to meet the gathering and transportation requirements. In such cases, tubing must be inserted to improve the liquid accumulation situation in the wellbore, transforming the liquid-laden production into liquid-carrying production, thereby reducing the energy loss in the wellbore.

Based on the established wellbore pressure drop calculation model, the pressure drop equation is:

$$\begin{cases} q_{sc} > q_c : \frac{d_p}{d_z} = \rho_m g + f_m \frac{G_m^2}{2DA^2\rho_m} \\ q_{sc} < q_c : \frac{d_p}{d_z} = \rho_m g \sin\theta + f_m \frac{\rho_m v_m^2}{2D} + f_m v_m \frac{d_{v_m}}{d_z} \end{cases} \quad (10)$$

In the equation, the first term on the right-hand side represents the gravity loss term, the second term represents the friction loss term, and the third term represents the acceleration loss term.

Among these, the acceleration loss term can be neglected. The friction loss is divided into gas-phase loss and liquid-phase loss. When the gas production rate is low, the friction loss is due to gas-liquid slip, which decreases as the gas production rate increases. When the gas production rate is high, the friction loss is caused by the friction between the gas and the pipe wall, which increases with the increase in gas production rate.

During casing production, the bottomhole flowing pressure equals the surface casing pressure + wellbore energy loss.

$$p_{wf1} = p_c + \triangle p_1 \quad (11)$$

After inserting the tubing, the surface tubing pressure equals the bottomhole flowing pressure minus the wellbore energy loss.

$$p_t = p_{wf2} - \triangle p_2 \quad (12)$$

Assuming that the gas and water production remain the same before and after inserting the tubing, and the formation pressure is the same (i.e., the production pressure difference and bottomhole flowing pressure are the same), the above equations can be combined to obtain the wellhead pressure after inserting the tubing:

$$p_t = p_c + (\triangle p_1 - \triangle p_2) \quad (13)$$

Taking Well Q1 as an exa mple, before inserting the tubing, the casing pressure was 3.53 MPa, gas production was 44,000 m³/day, and water production was 111 m³/day. After inserting the 2 3/8-inch tubing, the tubing pressure was 2.5 MPa, gas production was 39,000 m³/day, water production was 113 m³/day, and the wellhead pressure decreased by 1.0 MPa after inserting the tubing. The wellhead pressure variation curves were plotted for gas production rates of 30,000 m³/day and 50,000 m³/day after inserting the 2 3/8-inch tubing. The actual data from Well Q1 was substituted into the model to verify its accuracy. As can be seen, the curve positions (as shown in Fig. 11) closely match the actual wellhead pressure changes observed after inserting the tubing, indicating good accuracy.

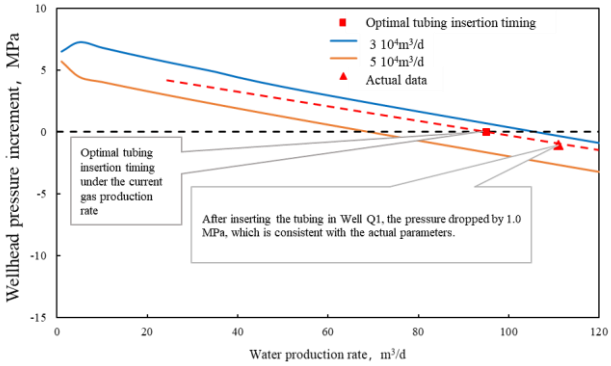

Fig. 11. Example analysis of the wellhead pressure change model of well Q1

5- Conclusion

This paper investigates the deep coalbed methane blocks in the Erdos region of the Changqing Oilfield. A thorough analysis was conducted on the production characteristics, backflow characteristics, and flow regime classification of deep coalbed methane. In response to the findings, engineering measures were implemented, including the optimization of tubing insertion timing and insertion angles. These measures effectively addressed current technical challenges and provided a solid scientific basis and technical support for the future management and development of the gas reservoir, ensuring that gas wells operate under optimal conditions. Based on the above research and practice, the following conclusions are drawn:

1) Deep and ultra-deep coalbed methane wells contain large amounts of methane, with a high proportion of free gas, and exhibit high initial water production. These wells have the characteristics of rapid drainage and early gas appearance. Based on these production characteristics, the production process can be divided into five stages: the pure-liquid production stage after fracturing, the gas-increase-and-water-increase stage, the gas-increase-and-water-decrease stage, the gas-decrease-and-water-decrease stage, and the stable production to depletion stage.

2) The backflow patterns of deep coalbed methane wells can be studied using a binomial model. If sufficient data is available, future researchers can classify gas wells based on the binomial coefficients A and B to analyze the production characteristics of coalbed methane wells under different backflow patterns.

3) Through the flow regime analysis of Well Q1, it was found that in the vertical section, the flow regime transitions from bubble flow → slug flow in the early stage, and with the reduction in water production, it is predicted to evolve from transition flow → annular flow in the later stage. In the inclined section, the flow regime is predominantly slug flow for most of the time. In the horizontal section, during the early stage, the flow transitions from elongated bubble flow → slug flow, in the middle stage from elongated bubble flow → stratified smooth flow, and in the later stage, it remains in the stratified smooth flow regime.

4) Through the optimization of the preferred tubing string design for Well Q1, it is determined that the insertion depth of the tubing for Well Q1 should be around 3600.0 m, and the tubing string should ideally be inserted when the water production is approximately 100 m^3/day.

Acknowledgement

The author would like to express sincere gratitude to the management of the Petroleum and Gas Technology Research Institute of Changqing Oilfield for authorizing the data support provided in this paper. Additionally, the author extends heartfelt thanks to the technical personnel who provided technical support during the field experiments.

Compliance with Ethical Standards Section

• Disclosure of potential conflicts of interest: There are no conflicts of interest.

• Research involving Human Participants and/or Animals: Not applicable.

• Informed consent: There is informed consent in publishing this research.

References

[1] T. E. Crist, C. M. Boyer, and B. S. Kelso, "A Geologic and Coalbed Methane Resource Analysis of the Menefee Formation in the San Juan Basin, Southwestern Colorado and Northwestern New Mexico," in *Low Permeability Reservoirs Symposium*, 1989, vol. Low Permeability Reservoirs Symposium, SPE-18945-MS. https://doi.org/10.2118/18945-MS

[2] A. H. Jones *et al.*, "Methane Production Characteristics for a Deeply Buried Coalbed Reservoir in the San Juan Basin," in *SPE Unconventional Gas Recovery Symposium*, 1984, vol. SPE Unconventional Gas Recovery Symposium, SPE-12876-MS. https://doi.org/10.2118/12876-MS

[3] K. J. Johnson, A. Coats, and S. A. Marinello, "Gas-Lift Technology Applied to Dewatering of Coalbed Methane Wells in the Black Warrior Basin," *SPE Production Engineering*, vol. 7, no. 04, pp. 379-383, 1992. https://doi.org/10.2118/21590-PA

[4] J. Misselbrook and K. Falk, "A Novel Method Using Coiled Tubing for Dewatering Gas Wells," in *SPE/ICoTA Coiled Tubing Conference and Exhibition*, 2005, vol. SPE/ICoTA Coiled Tubing Conference and Exhibition, SPE-94193-MS. https://doi.org/10.2118/94193-MS

[5] M. J. Willis and G. A. Conrad, "Reverse Osmosis Compatible Chemical Foamers For Gas Well Deliquification And Production Enhancement," in *SPE Asia Pacific Oil and Gas Conference and Exhibition*, 2010, vol. SPE Asia Pacific Oil and Gas Conference and Exhibition, SPE-133517-MS. https://doi.org/10.2118/133517-MS

[6] F. E. Trevisan and M. G. Prado, "Experimental Investigation on the Viscous Effect on Two-Phase Flow Patterns and Hydraulic Performance of Electrical Submersible Pumps," in *Canadian Unconventional Resources and International Petroleum Conference*, 2010, vol. Canadian Unconventional Resources and International Petroleum Conference, SPE-134089-MS. https://doi.org/10.2118/134089-MS

[7] T. Denney, B. Wolfe, and D. Zhu, "Benefit Evaluation of Keeping an Integrated Model During Real-Time ESP Operations," in *SPE Digital Energy Conference*, 2013, vol. SPE Digital Energy Conference, SPE-163704-MS. https://doi.org/10.2118/163704-MS

[8] D. B. Sarmiento Varela, M. Monroy Barrios, A. Gil Chacon, L. Luna, and A. Buitrago, "Successful Strategy through Artificial Lift Systems to Develop Coalbed Methane Production in Colombia," in *SPE Artificial Lift Conference-Americas*, 2013, vol. All Days, SPE-165047-MS. https://doi.org/10.2118/165047-MS

[9] G. Han, K. Ling, and H. Zhang, "Smart De-Watering and Production System through Real-Time Water Level Surveillance for Coal-Bed Methane Wells," in *Journal of Natural Gas Science and Engineering*, 2016, vol. 31. https://doi.org/10.1016/j.jngse.2016.03.075

[10] J. Vora, R. Singh, and S. Saxena, "Novel Idea for Optimization of a Progressive Cavity Pump PCP System at Different Stages of Coal Bed Methane CBM Well Life," in *SPE Oil and Gas India Conference and Exhibition*, 2017, vol. SPE Oil and Gas India Conference and Exhibition, D021S009R005. https://doi.org/10.2118/185380-MS

[11] C. Prosper and D. West, "Case Study Applied Machine Learning to Optimise PCP Completion Design in a CBM Field," in *SPE Asia Pacific Oil and Gas Conference and Exhibition*, 2018, vol. SPE Asia Pacific Oil and Gas Conference and Exhibition, D021S016R002. https://doi.org/10.2118/192002-MS

[12] C. Ejim and J. Xiao, "Screening Artificial Lift and Other Techniques for Liquid Unloading in Unconventional Gas Wells," in *Abu Dhabi International Petroleum Exhibition & Conference*, 2020, vol. Day 4 Thu, November 12, 2020, D041S103R002. https://doi.org/10.2118/202653-MS

[13] D. B. Larson, Y. Gogenhan, H. S. Parhar, G. A. A. Gonzalez, D. E. Salicas, and A. Boonstra, "Smart-Pump™ Methodology for Progressing Cavity Pump Sizing," in *SPE Artificial Lift Conference and Exhibition - Americas*, 2024, vol. SPE Artificial Lift Conference and Exhibition - Americas, D021S007R003. https://doi.org/10.2118/219540-MS

[14] S. K. Sharan and V. H. Keswani, "Successful Field Trial of Well Completion with Suitable Artificial Lift in Cbm Horizontal Wells of India," in *SPE Artificial Lift Conference and Exhibition - Americas*, 2024, vol. SPE Artificial Lift Conference and Exhibition - Americas, D021S007R005. https://doi.org/10.2118/219551-MS

تحليل خصائص الانتاج والتدابير الهندسية لابار الميثان العميقة في طبقات الفحم في حوض اوردوس

تشاو تشنغيانا [١، ٣، *]، تان شيا [٢]، وانغ شيانوينك [٣]، تيان ويك [٣]، جيا يوليانغك [٣]

١ كلية هندسة البترول، جامعة شيان شيبو، ٧١٠٠٦٥، الصين

٢ مختبر الدولة الرئيسي للجيولوجيا واستغلال مكامن النفط والغاز، جامعة جنوب غرب البترول، طريق شيندو ٨، تشنغدو ٦١٠٥٠٠، الصين .

٣ مركز ابحاث الهندسة لتطوير وادارة مكامن النفط والغاز ذات النفاذية المنخفضة الى المنخفضة للغاية في غرب الصين، وزارة التعليم، شيان، ٧١٠٠٦٥، الصين

الخلاصة

نظرًا للاختلافات الكبيرة في أنماط تراكم الغاز وخصائص خزان الفحم وظروف حفظ الغاز للميثان في طبقة الفحم العميقة للغاية (العمق الرأسي > ٣٠٠٠ متر، العمق المقاس > ٥٠٠٠ متر)، فإن خصائص إنتاجه وأنماط التدفق العكسي وتصنيفات مراحل التدفق تختلف أيضًا بشكل كبير. بالإضافة إلى ذلك، هناك قيود في تقنيات الإنتاج المطبقة على الخزانات العميقة. لاستكشاف العلاقة بين خصائص إنتاج ميثان طبقة الفحم العميقة وميثان طبقة الفحم المتوسطة ، وكذلك للتحقيق في التقنيات المناسبة لميثان طبقة الفحم العميقة، تستخدم هذه الورقة بئر Q1 كمثال وتجري بحثًا وتحليلًا بناءً على نظرية هندسة الخزان. يُعتقد أنه في المقطع الرأسي لبئر Q1 (العمق أقل من ٣٠٠٠ متر بشكل عام)، ينتقل نمط التدفق من التدفق الفقاعي إلى التدفق البطيء في المرحلة المبكرة، ومع انخفاض إنتاج المياه، من المتوقع أن ينتقل من التدفق الانتقالي إلى التدفق الحلقي في المرحلة اللاحقة. في المقطع المائل (يتراوح العمق عادةً بين ٣٠٠٠ و٤٠٠٠ متر)، يسود تدفق الرغوة في معظم الأوقات، بينما في المقطع الأفقي (يتجاوز العمق عادةً ٤٠٠٠ متر)، يتطور التدفق من تدفق فقاعي ممتد إلى تدفق رغوي في المرحلة المبكرة، ومن تدفق فقاعي ممتد إلى تدفق سلس طبقي في المرحلة الوسطى، ويبقى في منطقة التدفق السلس الطبقي في المرحلة اللاحقة. علاوة على ذلك، يُقترح ربط عمق إدخال البئر Q1 بزاوية انحراف البئر، ومعدل إنتاج الغاز، ومعدل إنتاج الماء. ومن منظور تحسين نسبة الغاز إلى الماء وكفاءة الطاقة، يجب أن يكون هناك توقيت مثالي لإدخال الأنابيب.

الكلمات الدالة: غاز الميثان في طبقات الفحم العميقة، نظام الإنتاج، نمط الإنتاج، التدابير الهندسية، تحليل التدفق العكسي، التنبؤ بنمط التدفق.